URSI GASS 2021, Rome, Italy, 28 August - 4 September 2021

Systematically Characterizing Planetary Surface Roughness Using Spacecraft Radio Communications Antennas

Elizabeth M. Palmer[1] and Essam Heggy* [1,2]
(1) University of Southern California, Los Angeles, CA, USA 90089-0271
(2) NASA Jet Propulsion Laboratory, California Institute of Technology, Pasadena, CA, USA 91109

Abstract

Mapping the surface roughness of a planetary body at centimeter-to-decimeter (cm-dm) scales provides unique insights into the primary geophysical processes governing the surface's evolution and provides important input for accurate surface trafficability assessments for future lander, rover, and sample return missions. Toward these objectives, NASA's Dawn mission acquired opportunistic, bistatic radar (BSR) surface occultation observations of Asteroid Vesta, using the spacecraft communications antenna to transmit, and Deep Space Network (DSN) antennas to receive. Subsequent power spectral analysis of each forward-scattered surface echo ultimately yielded regional estimates of relative surface roughness at the cm-dm scale. Herein, we outline an opportunity for orbital and flyby missions to systematically characterize planetary surface roughness across the solar system by utilizing spacecrafts' X- and S-band onboard radio communications antennas to perform similar BSR observations. In addition, we present a newly developed user interface that automates the processing and analysis of raw DSN radio science datasets, hence enabling the broader planetary science community to utilize BSR data in characterizing the textural and electrical properties of planetary surfaces.

1 Introduction

Identifying the primary geophysical processes that have acted to shape a particular planetary surface, whether impact cratering, lava flows, volatile outgassing, or others, provides key insights into the body's formation and evolutionary history. Such processes can be inferred from the texture of the surface at sub-meter scales, and the degree to which this texture varies over the planetary body. On the Moon for example, its surface evolution is dominated by impact processes, resulting in smooth dusty regolith comprising the oldest terrain (abrasively eroded by continuous micrometeorite bombardment), and the occurrence of rough, blocky crater ejecta (associated with fresh craters) in the youngest terrain.

Accurately assessing the surface texture of planetary bodies at sub-meter scales is also crucial for characterizing surface trafficability in the case of future lander, rover, and sample return missions to these bodies. The Rosetta mission to Comet 67P, for example, found that the surface and shallow subsurface was far rockier and more fragmented at meter and sub-meter scales than expected after its lander Philae bounced several times from the comet's surface, away from its targeted landing site, eventually settling beneath the shadow of an overhang where it gradually lost its solar-powered charge [1, 2].

While the bulk of planetary surface geologic mapping is performed at topographic scales owing to the use of remote sensing images acquired by optical cameras aboard orbiting or flyby spacecraft (i.e., mapping features larger than a few meters), smaller-scale geomorphologic features are far less well characterized due to the trade-off between image resolution and surface area coverage. For instance, the HiRISE imager aboard the Mars Reconnaissance Orbiter has been acquiring sub-meter-resolution images at ~30 cm/pixel for the last 15 years, but its coverage only encompasses ~2% of the martian surface [3].

Herein, we discuss the capabilities of planetary radio science to opportunistically and systematically characterize the surface roughness of planetary bodies at cm-dm scales. We review past observations of surface roughness retrieved from BSR occultation observations, and discuss the technical challenges and potential outcomes associated with performing similar surface-scatter BSR observations of planetary surfaces in the future.

2 Surface Roughness Characterization by Planetary BSR Occultations

Radar remote sensing is particularly well-suited for characterizing surface texture at the sub-meter scale since the amplitude and phase of radar scatter from planetary surfaces depend primarily on (1) surface topography, (2) surface roughness at the scale of one-tenth to ten times the wavelength, and (3) the intrinsic dielectric properties of the surface material—which in turn depend primarily on density, mineralogy, dust-to-ice ratio, and temperature [4]. Hence, orbital radars operating in the range of 300 MHz (1 m wavelength) to 30 GHz (1 cm wavelength) can be used to infer surface roughness across a given body when topography and surface dielectric properties are well known. An opportunity arises then for orbital and flyby space missions to characterize cm-dm surface roughness using their radio communications antennas to perform bistatic radar (BSR) observations of the surface, as they generally operate at 4 cm and/or 13 cm wavelengths (X- and S-band radio frequencies, respectively).

An advantage of performing opportunistic BSR observations is that mission trajectories—and the allocation of time to other primary onboard science instruments—need not be altered, provided the occurrence of occasional occultations of the spacecraft behind the planetary object from Earth's perspective, as depicted in Fig. 1. In this configuration, using downlink mode as an example, the signal is continuously transmitted from the high-gain antenna directly toward Deep Space Network (DSN) ground stations, and as the spacecraft begins to enter or exit from an occultation, the transmitted radio waves are forward-scattered from the target's surface at grazing incidence, and received at the DSN for processing and analysis. By comparing the surface-scattered signal strength with that of the unimpeded direct carrier signal, one can infer surface reflectivity and from this infer surface roughness (when the dielectric properties of the surface material are known) or infer dielectric properties (when the surface roughness is known).

The BSR occultation technique has been performed by several space missions over the decades: at Mercury by MESSENGER [5], Venus by Magellan and Venus Express [6], the Moon by Lunar Orbiter I [7, 8], Mars by Mariner, Viking, the Mars Global Surveyor and Mars Odyssey [9, 8, 10, 11], Vesta by Dawn [12], Titan by the Cassini-Huygens probe [13], Comet 67P by Rosetta [14, 15] and Pluto by New Horizons [16]. Among these missions, the BSR experiment by Lunar Orbiter I observed the dichotomy of roughness between the lunar highlands and the maria at cm-dm scales [7]; the Viking mission observed characteristically different surface roughness for the martian plains (smoothest), sand dunes (roughest), and the polar caps (intermediate roughness) at cm-dm scales [17]; Mars Odyssey used its BSR observations to characterize variability in the smoothness of potential landing sites for the Phoenix mission at meter-to-multi-meter scales [11]; and BSR observations by Huygens provided the first in-situ assessment of surface roughness on Titan at the cm-dm scale [13].

At Asteroid Vesta, BSR observations by Dawn revealed a wide variability of cm-dm surface roughness that was not correlated with crater distribution or surface age, suggesting that impact processes alone could not explain its surface texture [12]. Extensive, relatively smoother areas were found to overlap with mapped observations of heightened subsurface hydrogen concentrations measured by the Gamma Ray and Neutron Detector aboard Dawn [18], suggesting that buried water-ice may have played a role in shaping of the asteroid's surface at the cm-dm scale in these regions [12].

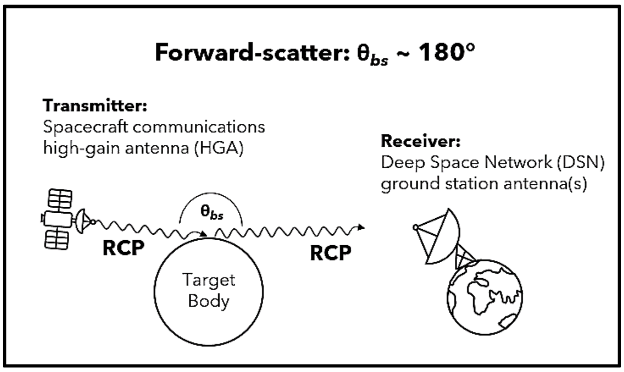

Figure 1. Observation geometry (not to scale) of an orbital forward-scatter bistatic radar experiment.

Interpreting Vesta's surface textural properties from the raw data took several years, however, owing to complex acquisition geometries around such a small body—where grazing incidence angles and a slow spacecraft orbit resulted in surface-scattered echoes with unexpectedly small Doppler shifts from the direct signal (the differential Doppler shift), making echoes difficult to identify in the raw data without using proper processing parameters specifically tailored to the mission [12, 19]. Similarly, Rosetta's BSR observations of Comet 67P remain unpublished owing to highly complex geometry around an irregularly-shaped small body that has yielded non-intuitive results [15].

3 Automating the Processing and Analysis of Raw DSN Radio Science Data

Given the complex observation geometries associated with planetary radio science observations, as well as the complexity of generating different data products from raw planetary radio science datasets and quantifying sources of error (as opposed to other planetary datasets that provide visual verification tools for data quality analysis, such as optical and spectroscopic imaging), subsequent processing, analysis and interpretation are often challenging and time-consuming [12, 15]. Hence, in spite of public availability of such data on NASA Planetary Data System archives or equivalent repositories, planetary radio science data products have largely been accessible only by experts [20].

To enable the broader planetary science community to utilize such BSR datasets to characterize the electrical and textural properties of planetary surfaces—including the ability to perform expedient, in-flight analysis of opportunistic BSR occultation—we have developed a publicly accessible user interface called "PARSE" (Processing and Analysis for Radio Science Experiments), Fig. 2, that automates the data processing chain initially developed for Dawn's BSR observations of Vesta [12]. PARSE also calculates the theoretical value of the differential Doppler shift (between the direct signal and

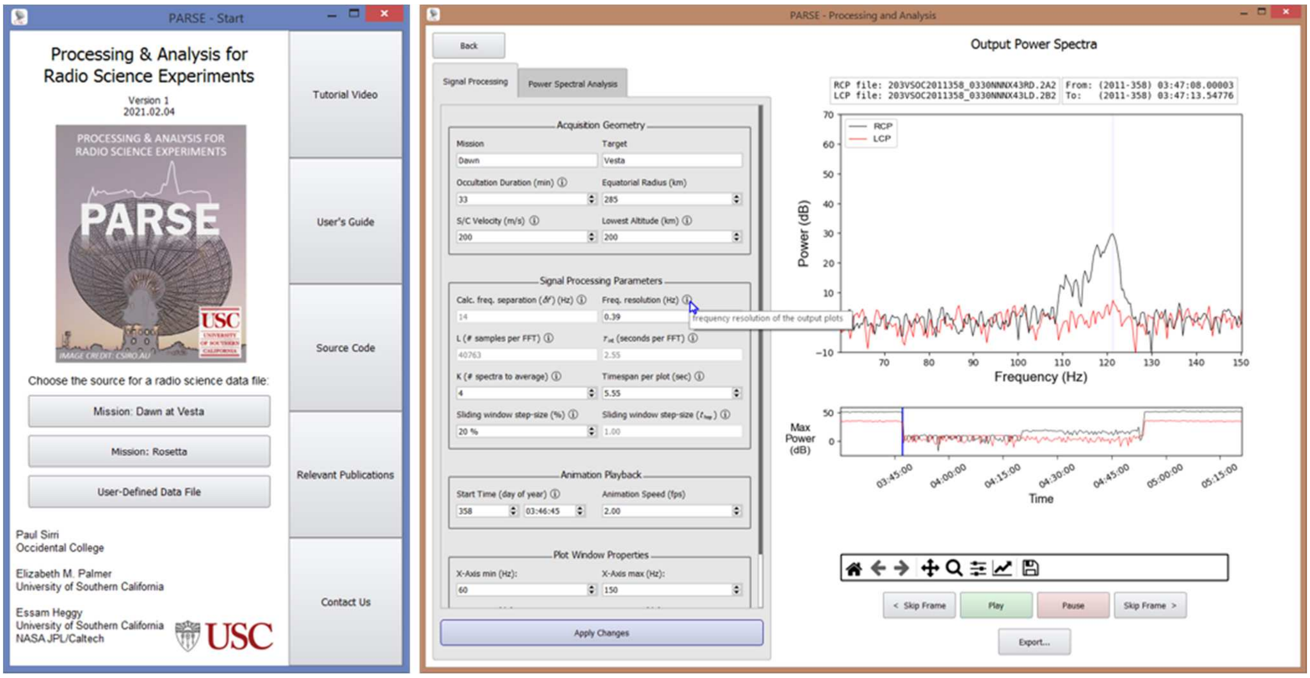

Figure 2. Screenshots of publicly-accessible PARSE tool (Processing and Analysis for Radio Science Experiments). *(Left)* Start screen. *(Right)* Adjustable signal processing parameters, and subsequent power spectral diagram (as a playable video displaying changes in signal strength and bandwidth over time).

any surface echoes) by applying the algorithm of [19] to the mission's specific observation geometry, from which PARSE suggests nominal signal processing parameters.

4 Technical Challenges and Future Prospects

Considering the current frequency stabilities associated with onboard, internal auxiliary oscillators for one-way spacecraft communications [e.g., 21], Palmer and Heggy [19] find that the above-described opportunistic BSR occultation observations of planetary surfaces are feasible for orbital missions at planetary bodies ≥100 km in diameter, as the orbital velocity of the spacecraft will be sufficiently large to induce a measurable differential Doppler shift between the surface-scattered signal and the direct signal, which in turn is necessary for accurately retrieving surface radar reflective properties from power spectral analysis of the surface-scattered signal.

Missions equipped with onboard ultra-stable oscillators (USOs) on the other hand, are able to perform BSR occultation observations of small-bodies, such as asteroids and comets, that are ≤100 km in diameter, such as the BSR experiment by Rosetta at Comet 67P [14, 15, 21, 22]. The more frequently that spacecraft are equipped with USOs, or as the frequency stability requirements for internal auxiliary oscillators increases, the more planetary surfaces that can be characterized by the BSR occultation technique, thereby establishing a larger database of surface roughness characteristics. Other prospects for advancement in bistatic radar observations of planetary surfaces includes the use of two or more orbiting spacecraft around a single planetary object, thereby enabling a much larger range of bistatic incidence angles over which to observe a given surface, such as the BepiColombo mission to Mercury [23].

Overall, building a much larger pool of high-incidence-angle BSR observations of different planetary bodies will enable us to assess: (1) the primary geophysical processes that act to shape different types of planetary objects in the solar system, such as small-bodies, moons and the terrestrial planets; (2) whether or not cm-dm-scale surface roughness variability correlates with optically-observed surface features; and (3) safe surface trafficability, thereby enabling identification of nominally smooth sites for future landing, roving or sample return missions. Through this magnitude of data collection, a statistical picture can be formed in understanding the relationship between the roughness of different planetary surfaces, and what physical processes have contributed to their shaping.

4 Acknowledgements

The authors thank Paul Sirri (Occidental College; USC) for designing and implementing the PARSE user interface. This work is funded by the University of Southern California (USC) under the NASA Planetary Geology and Geophysics (PGG) program, grant WBS 811073.02.01.07.05, awarded to Heggy; and under the NASA Jet Propulsion Laboratory (JPL) award to Heggy (005608-00001/Prime No: NNN12AA01C).

5 References

1. S. Ulamec *et al.*, “Rosetta Lander – Philae: Landing preparations,” *Acta Astronaut.*, **107**, pp. 79–86, Feb. 2015, doi:10.1016/j.actaastro.2014.11.019.

2. S. Ulamec *et al.*, “Rosetta Lander - Philae: Operations on comet 67P/Churyumov-Gerasimenko, analysis of wake-up activities and final state,” *Acta Astronaut.*, **137**, pp. 38–43, Aug. 2017, doi:10.1016/j.actaastro.2017.04.005.

3. S. McEwen and the HiRISE Science and Operations Team, “The Future of MRO/HiRISE,” presented at the Lunar Planet. Sci. Conf., Houston, TX, 2018, **49**, Abstract #1301.

4. B. A. Campbell, *Radar Remote Sensing of Planetary Surfaces*. Cambridge University Press, 2002.

5. M. E. Perry *et al.*, “Measurement of the radius of Mercury by radio occultation during the MESSENGER flybys,” *Planet. Space Sci*., **59**, 15, pp. 1925–1931, 2011, doi:10.1016/j.pss.2011.07.022.

6. R. A. Simpson, G. L. Tyler, B. Häusler, R. Mattei, and M. Pätzold, “Venus Express bistatic radar: High-elevation anomalous reflectivity,” *J. Geophys. Res.*, **114**, 2009, doi:10.1029/2008JE003156.

7. G. L. Tyler, V. R. Eshleman, G. Fjeldbo, H. T. Howard, and A. M. Peterson, “Bistatic-Radar Detection of Lunar Scattering Centers with Lunar Orbiter I,” *Science*, **157**, 3785, pp. 193–195, 1967, doi:10.1126/science.157.3785.193.

8. R. A. Simpson, “Spacecraft studies of planetary surfaces using bistatic radar,” *IEEE Trans. Geosci. Remote Sens.*, **31**, 2, pp. 465–482, 1993, doi:10.1109/36.214923.

9. G. Fjeldbo, A. Kliore, and B. Seidel, “Bistatic radar measurements of the surface of Mars with Mariner 1969,” *Icarus*, **16**, 3, pp. 502–508, 1972, doi:10.1016/0019-1035(72)90096-6.

10. R. Simpson and G. L. Tyler, “Mars Global Surveyor Bistatic Radar Probing of the MPL/DS2 Target Area,” *Icarus*, **152**, 1, pp. 70–74, 2001, doi:10.1006/icar.2001.6629.

11. H. M. Gunnarsdottir, I. R. Linscott, J. L. Callas, M. D. Cousins, R. A. Simpson, and G. L. Tyler, “Root-mean-square surface slopes of Phoenix landing sites with 75-cm bistatic radar received by Mars Odyssey,” *J. Geophys. Res.,* **113**, p. E00A02, 2008, doi:10.1029/2007JE003040.

12. E. M. Palmer, E. Heggy, and W. Kofman, “Orbital bistatic radar observations of asteroid Vesta by the Dawn mission,” *Nat. Commun.*, **8**, 409, pp. 1–12, 2017, doi:10.1038/s41467-017-00434-6.

13. M. Pérez-Ayúcar, R. D. Lorenz, N. Floury, R. Prieto-Cerdeira, and J.-P. Lebreton, “Bistatic observations of Titan’s surface with the Huygens probe radio signal,” *J. Geophys. Res. Planet.,* **111**, E7, 2006, doi:10.1029/2005JE002613.

14. M. Pätzold *et al.*, “Rosetta Radio Science Investigations (RSI),” *Space Sci Rev*, **128**, 1–4, pp. 599–627, 2007, doi:10.1007/s11214-006-9117-7.

15. G. G. Peytaví *et al.*, “Processing Bistatic Radar Observations of Comet 67P/Churyumov-Gerasimenko,” presented at the 49th Rosetta Science Team Meeting, Rhodes, Greece, 2018.

16. D. P. Hinson *et al.*, “Radio occultation measurements of Pluto’s neutral atmosphere with New Horizons,” *Icarus*, **290**, pp. 96–111, 2017, doi:10.1016/j.icarus.2017.02.031.

17. R. A. Simpson and G. L. Tyler, “Viking bistatic radar experiment: Summary of first-order results emphasizing north polar data,” *Icarus*, **46**, 3, pp. 361–389, 1981, doi:10.1016/0019-1035(81)90139-1.

18. T. H. Prettyman *et al.*, “Elemental Mapping by Dawn Reveals Exogenic H in Vesta’s Regolith,” *Science*, **338**, 6104, pp. 242–246, 2012, doi:10.1126/science.1225354.

19. E. M. Palmer and E. Heggy, “Bistatic Radar Occultations of Planetary Surfaces,” *IEEE Geosci. Remote Sensing Lett.*, **17**, 5, pp. 804–808, 2020, doi:10.1109/LGRS.2019.2931310.

20. P. Withers, L. Moore, K. Cahoy, and I. Beerer, “How to process radio occultation data: 1. From time series of frequency residuals to vertical profiles of atmospheric and ionospheric properties,” *Planet. Space Sci.*, **101**, pp. 77–88, 2014, doi:10.1016/j.pss.2014.06.011.

21. C.-C. Chen *et al.*, Small Deep Space Transponder (SDST) DS1 Technology Validation Report, document JPL Publication 00-1011, 2000, pp. 1–26.

22. S. W. Asmar, J. W. Armstrong, L. Iess, and P. Tortora, “Spacecraft Doppler tracking: Noise budget and accuracy achievable in precision radio science observations,” *Radio Sci.*, **40**, 2, pp. 1–9, 2005, doi:10.1029/2004RS003101.

23. J. Benkhoff *et al.*, “BepiColombo—Comprehensive exploration of Mercury: Mission overview and science goals,” *Planet. Space Sci.*, **58**, 1, pp. 2–20, 2010, doi:10.1016/j.pss.2009.09.020.